

Data-Driven Model Identification via Hyperparameter Optimization for Autonomous Racing Systems

Hyunki Seong¹, Chanyoung Chung^{2*}, and David Hyunchul Shim¹

Abstract—In this letter, we propose a model identification method via hyperparameter optimization (MIHO). Our method adopts an efficient explore-exploit strategy to identify the parameters of dynamic models in a data-driven optimization manner. We utilize MIHO for model parameter identification of the AV-21, a full-scaled autonomous race vehicle. We then incorporate the optimized parameters for the design of model-based planning and control systems of our platform. In experiments, the learned parametric models demonstrate good fitness to given datasets and show generalization ability in unseen dynamic scenarios. We further conduct extensive field tests to validate our model-based system. The tests show that our race systems leverage the learned model dynamics and successfully perform obstacle avoidance and high-speed driving over 200km/h at the Indianapolis Motor Speedway and Las Vegas Motor Speedway. The source code for MIHO and videos of the tests are available at <https://github.com/hynkis/MIHO>.

Index Terms—Data-driven control, hyperparameter optimization, autonomous vehicle

I. INTRODUCTION

Understanding the system model is essential for robotic applications, especially safety-critical autonomous systems. In particular, at high-speed driving, various dynamics elements such as chassis, tires, or engines become crucial to implement high-speed autonomy. Model-based optimal control [1], [2] is well-suited for handling those factors and is widely used to design dynamics system control. By leveraging physics-based parametric dynamic models, it optimizes driving behavior with respect to a designed objective function and enables safe and reliable control system design.

Despite the success of the model-based approach in robotics, the model-based algorithm has two fundamental challenges: model fidelity and tractability. The performance of model-based approaches relies heavily on the accuracy of the model. However, identifying accurate models is often laborious or

This work was supported by Institute of Information communications Technology Planning Evaluation (IITP) grant funded by the Korea government(MSIT) (2021-0-00029, Development of Indoor Autonomous Drone for Performing Multiple Missions Based on Artificial Intelligence)

*Corresponding author

¹ The authors are with the School of Electrical Engineering, Korea Advanced Institute of Science and Technology, Daejeon, South Korea. (email: hynkis@kaist.ac.kr;geninfty@kaist.ac.kr)

² Chanyoung Chung is with the JPL Science Division, NASA, California, USA. (email: chanyoung.chung@jpl.nasa.gov)

intractable because of their large search space and nonlinearity. Other than the model accuracy, models also need to be computationally feasible for the real-time control applications. High-fidelity but highly complex models are often difficult to integrate into real-time safety-critical driving systems.

To tackle these challenges, conventional approaches, including the Prediction Error Method, are used to identify model parameters [3]. However, those methods often require the model structure to be linear or in specific mathematical forms, which might not be feasible to describe the nonlinear high-speed autonomous driving system. On the other hand, in several recent works, data-driven approaches using neural networks, Gaussian processes, or Bayesian methods have been actively employed for nonlinear system dynamics modeling and have shown promising results [4]. In [5], they proposed a simple neural network to replace a single-track vehicle model and used it to generate feedforward control signals. Similarly, in [6], they designed Deep Neural Networks (DNN) as a model approximator to identify the vehicle dynamics model in an end-to-end learning fashion. However, while DNN is an efficient way to approximate nonlinear systems, it is difficult to integrate with non-learning model-based methods, which are reliable in real-world applications. Furthermore, it is challenging to ensure the validity of the DNN model in unseen driving scenarios without large-scale field tests.

In this letter, we propose a data-driven model identification method via hyperparameter optimization (MIHO) for high-speed autonomous racing systems. Our key idea is to leverage a parameter optimization approach from machine learning to identify physics-based parametric models in a data-driven manner without any limitation on the form of the model equation. To this end, we adopt a novel hyperparameter optimization (HPO) method that has an efficient exploration and exploitation strategy. Using the proposed method, we estimate the parameters of the integrable parametric dynamics models for a full-scaled autonomous racecar platform, Dallara AV-21 (Fig. 1), at the Indy Autonomous Challenge (IAC) [7]. We validate our proposed approach by integrating identified models into the high-speed autonomous system and conducting extensive field experiments, including over 200km/h autonomous driving and obstacle avoidance scenarios in the Indianapolis Motor Speedway (IMS) and Las Vegas Motor Speedway (LVMS).

In summary, our technical contributions are as follows:

- We propose a data-driven model identification method via hyperparameter optimization.
- We design model-based planning and control systems incorporating the learned vehicle dynamics models.
- We integrate the systems with learned model parameters into the full-scaled autonomous race vehicle and extensively validate them during the IAC.

II. MODEL IDENTIFICATION VIA HYPERPARAMETER OPTIMIZATION

Vehicle dynamic models allow us to describe the race vehicle's motion accurately. However, dynamics models with high fidelity are often challenging to identify due to their high nonlinearity and a large number of model parameters. Therefore, an efficient parameter estimation approach is necessary to find the parameter configuration of such complex models. In this letter, we propose a model identification method via hyperparameter optimization (MIHO) to learn the optimal model parameter configuration by a data-driven approach. Hyperparameter optimization (HPO) is the problem of selecting an optimal hyperparameter configuration required for neural network training in the machine learning field [8]. A hyperparameter is a parameter that controls the training process. HPO optimizes the hyperparameter configuration by evaluating the performance of the configuration during the model training process. Since one course of neural network training requires a substantial time, HPO focuses on the balanced exploration and exploitation strategy for the efficient optimal hyperparameter selection. [8]. Motivated by the balanced strategy, we design MIHO by adopting the HPO to the model identification problem. First, we regard a parameter configuration $p \in \mathbb{R}^{n_p}$ with n_p model parameters as a set of hyperparameters of a nonlinear dynamics model f . Then, we identify the parameter configuration by evaluating the following objective function inspired by the standard supervised learning problem:

$$\mathcal{L} = \frac{1}{|D|} \sum_{(x,y) \in D} \|y - f(x; p)\|^2, \quad (1)$$

where x, y denote the sampled input and output data of the model f from a given dataset D . By minimizing this learning objective, we find an optimized model parameter configuration p^* that has the minimum model error with the observed model output y . The model f has no limitation on its form

Algorithm 1 MIHO Algorithm based on Hyperband

Input: R, η, D

```

1:  $s_{max} \leftarrow \lfloor \log_\eta(R) \rfloor, B = (s_{max} + 1)R$ 
2: for  $s \in \{s_{max}, s_{max} - 1, \dots, 0\}$  do
3:    $n = \lceil \frac{B}{R} \frac{\eta^s}{(s+1)} \rceil, r = R\eta^{-s}$ 
4:    $P = \text{get\_model\_param\_config}(n)$ 
5:   for  $j \in \{0, \dots, s\}$  do
6:      $n_j = \lfloor n\eta^{-j} \rfloor, r_j = r\eta^j$ 
7:      $L = \{\text{eval\_with\_mutation}(p, r_j, D) : p \in P\}$ 
8:      $P = \text{select\_top\_k\_config}(P, L, \lfloor n_j/\eta \rfloor)$ 

```

Output: Optimized parameters p^* with the smallest loss.

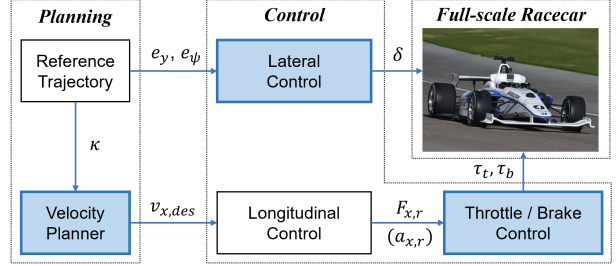


Fig. 1. Overview of our autonomous driving system in the AV-21. Our learned model parameters are embedded in the planning and control modules that are covered in this letter (highlighted in blue). Several input variables are omitted for clarity.

of the equation. Thus, our method can be used for arbitrary parametric models, such as a combination of polynomial or mathematical terms, as well as analytic physics-based models.

We implement MIHO incorporating a bandit-based HPO algorithm, Hyperband [9], as summarized in Algorithm 1. It is a variation of a random search algorithm with explore-exploit theory to find the optimal hyperparameter configuration based on an evaluation loss. The algorithm needs two arguments: R , the maximum amount of resource (e.g., the number of evaluation iterations) that can be allocated to a single configuration, and η , a value that determines the proportion of the discarded configurations. The two arguments derive $s_{max} + 1$ combinations (called "brackets" in [9]) of the values n and r , which enables various ratios of exploration and exploitation for finding the optimal parameter configuration. Hyperband compares the evaluation loss of each sampled configuration and allocates more resources to the configurations with lower evaluation losses, excluding the configurations with higher losses. It repeats the sampling and exclusion processes until the last configuration remains to obtain the optimal set of hyperparameters. To adjust the HPO algorithm to the model parameter optimization, we add the Gaussian mutation [10] during the evaluation to explore the new neighbor parameters that might have less model loss. Unlike the original HPO, which only allocates more resources r_i , our approach, MIHO, adds noise perturbation with a noise random variable $\epsilon \in \mathbb{R}^{n_p}$ at the selected configuration p after the resource allocation as:

$$p_{mut} = p + \sigma \odot \epsilon, \quad \epsilon \sim N(0, I), \quad (2)$$

where \odot is the element-wise product and $\sigma \in \mathbb{R}^{n_p}$ is the standard deviation of the exploration noise that is annealed over the course of the evaluation [11]. We define the following three functions for the HPO process in MIHO:

- *get_model_param_config(n)*: a function that returns a set of n random parameter configurations from the normal distribution pre-defined over the configuration space.
- *eval_with_mutation(p, r_j, D)*: a function that receives a parameter configuration p , an allocated resource r_j , and a dataset D as arguments. Using the dataset, this function evaluates an initial configuration and mutates it for the allocated r_j iterations by Eq. 2. If a mutated configuration $p_{mut} \in \mathbb{R}^{n_p}$ has a less loss than the initial one, the function replaces p with p_{mut} . It returns the final loss after spending the allocated resources.
- *select_top_k_config(P, L, k)*: a function that receives a

set of hyperparameter configurations P with their corresponding evaluation losses L and returns the top k high-performing configurations (here, $k = \lfloor n_j / \eta \rfloor$).

III. VEHICLE DYNAMICS MODEL

A. Tire Dynamics Model

Tire dynamics is one of the factors that significantly affect the nonlinearity of driving dynamics. Especially the lateral tire model is crucial to design stable path-tracking control in high-speed driving. The tire model [12] can be described as a function of the slip angle α_i , slip ratio $\rho_{x,i}$, inclination angle θ_i , tire load $F_{z,i}$, and current velocity $v_{x,i}$, which has a lateral tire force $F_{y,i}^*$ of each tire ($i \in \{LF, LR, RF, RR\}$) as,

$$F_{y,i}^* = f_{tire}(\alpha_i, \rho_{x,i}, \theta_i, F_{z,i}, v_{x,i}). \quad (3)$$

Although the model has high fidelity with various dynamics perspectives, it has low suitability for designing the controller of high-speed driving, which requires real-time performance. Therefore, we first define a tire model with dimension-reduction that can be applied to model-based control design within an acceptable complexity. We then optimize the model's parameter configuration to represent the overall tire characteristic of a given dataset using our MIHO algorithm. We follow the Pacejka tire model [13] to define the tire dynamics. While the prior work neglect vertical and horizontal offsets of the model, we formulate a tire model $F_{y,i} = f_{t,i}(\alpha_i; p_{t,i})$ containing the offset parameters $S_{x,i}, S_{y,i}$ to describe the asymmetric tire characteristic determined to maximize cornering performance on an oval track:

$$F_{y,i} = D_i \sin(C_i \arctan(B_i(\alpha_i + S_{x,i}))) + S_{y,i}, \quad (4)$$

where the tire model parameter configuration $p_{t,i} = \{B_i, C_i, D_i, S_{x,i}, S_{y,i}\}$ is identified by minimizing the following tire model objective with a given dataset $D_{t,i}$ as

$$\mathcal{L}_{t,i} = \frac{1}{|D_{t,i}|} \sum_{(\alpha_i, F_{y,i}^*) \in D_{t,i}} \|F_{y,i}^* - f_{t,i}(\alpha_i; p_{t,i})\|^2. \quad (5)$$

B. Engine Torque Model

The powertrain system of our racecar consists of an internal combustion engine, transmission, and wheels. The AV-21 is a rear-wheel-drive vehicle whose traction force $F_{x,r}$ is generated by engine-based driveline dynamics. We model the equation of the longitudinal dynamics [14] as follows:

$$ma_x = F_{x,r} - C_d v_x^2 - C_r, \quad (6)$$

where m is the vehicle mass, v_x is the longitudinal velocity, C_d denotes the drag coefficient, and C_r denotes the rolling resistance. Following a prior work [15], the traction force can be expressed as:

$$F_{x,r} = ma_{x,r} = \frac{T_e \eta_t i_g i_0}{R_w}, \quad (7)$$

where $a_{x,r}$ denotes the traction acceleration, η_t denotes the efficiency of the transmission, i_g, i_0 denote the transmission ratio of the current gear and final reducer, and R_w denotes the wheel radius. $T_e = f_e(w_e, \tau_t)$ is the engine torque map

in terms of the engine speed w_e and throttle command τ_t . Due to the high complexity of the engine characteristic, the torque map is expressed as an experimental lookup table based on engine torque curves of specific throttle opening commands. Although the engine torque model can be obtained by the engine dynamometer testing [16], it could suffer from modeling errors because the dynamometer testing is done in a static environment. Therefore, we build the engine torque map that integrates the dyno data with learned torque curves based on our data-driven model identification approach. We express an engine torque curve $T_{e,\tau_t} = f_{\tau_t}(w_e; p_{\tau_t})$ of a throttle command τ_t as a third order polynomial function of the engine speed w_e as:

$$T_{e,\tau_t} = p_{\tau_t,0} + p_{\tau_t,1} w_e + p_{\tau_t,2} w_e^2 + p_{\tau_t,3} w_e^3, \quad (8)$$

where $p_{\tau_t} = \{p_{\tau_t,0}, p_{\tau_t,1}, p_{\tau_t,2}, p_{\tau_t,3}\}$ is the torque model parameter configuration. Using the resultant traction accelerations $a_{x,r}$ while driving, the engine torque output T_{e,τ_t}^* is obtained by Eq. 7. Then, p_{τ_t} is learned by minimizing the following engine model objective with a given dataset D_{τ_t} :

$$\mathcal{L}_{\tau_t} = \frac{1}{|D_{\tau_t}|} \sum_{(w_e, T_{e,\tau_t}^*) \in D_{\tau_t}} \|T_{e,\tau_t}^* - f_{\tau_t}(w_e; p_{\tau_t})\|^2. \quad (9)$$

To stabilize the learning process, we normalize the engine speed in the range [0,1] with the maximum engine speed.

IV. MODEL-BASED PLANNING AND CONTROL

In this session, we introduce a model-based planning and control algorithm that uses the learned model parameters. We exploit the learned tire parameters to design a dynamics-aware velocity planning and model-based lateral controller (Fig. 1). We also integrate the engine dyno data with the learned engine torque model to construct an engine lookup table.

A. Dynamics-aware Velocity Planning

High-speed cornering during racing causes significant tire load transfer on each wheel due to a lateral acceleration at the roll axis. Since the tire load governs the maximum performance of the tire, a model-based velocity strategy accounting for the real-time wheel load is necessary to maximize the tire performance without losing tire grip. We introduce a dynamics-aware velocity planning algorithm that derives the velocity plans with maximum tire performance based on the learned tire dynamics. We first compute the real-time vertical tire load $F_{z,i}$ affected by the lateral load transfer ΔW_f [17]. The diagram of the load transfer at the roll axis is illustrated in the left of Fig. 2. The load transfer is computed by the roll couple $C_{roll} = m_s \dot{v}_y h_a$, where m_s is the sprung mass, \dot{v}_y is the lateral acceleration, and h_a is the roll height. As the learned tire model describes the characteristic for the nominal tire load $\bar{F}_{z,i}$, we compute the maximum lateral force of each tire $F_{y,i}^{max}$ in terms of the tire load ratio with peak value of the tire model as:

$$F_{y,i}^{max} = \mu \frac{F_{z,i}}{\bar{F}_{z,i}} F_{y,i}^{peak}, \quad (10)$$

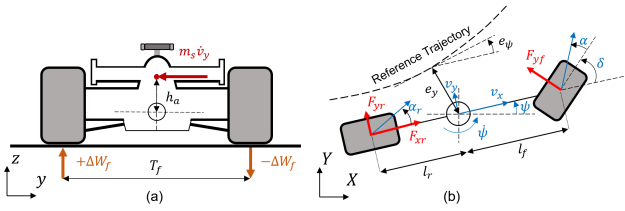


Fig. 2. Left: Lateral load transfer generation by the lateral acceleration at the roll axis. Right: Overall diagram of the vehicle model.

where μ is a tire performance factor to control the confidence and maximum performance of the tire model, $\frac{F_{z,i}}{F_{z,i}}$ is the tire load ratio. The maximum lateral acceleration is determined by the following lateral motion dynamics [13]:

$$a_{y,max} = \frac{1}{m} (F_{y,r}^{max} + F_{y,f}^{max} \cos(\delta) - mv_x \dot{\psi}), \quad (11)$$

where δ is the steering angle and $\dot{\psi}$ is the yaw rate. Then a desired maximum velocity $v_{x,des}$ is planned according to the curvature κ of a reference path from a planning module [18]:

$$v_{x,des} = \sqrt{a_{y,max}/\kappa}. \quad (12)$$

B. Throttle and Brake Control

The planned desired velocity is fed to a feedback control module [19] to compute the traction force. However, as shown in Fig 1, another low-level controller to transform the traction force to the throttle command is required to control the racecar with nonlinear driveline dynamics. We design the throttle and brake control system following [20]. Fig. 3 shows the details of the low-level control system. We exploit the integrated engine torque map to convert the desired engine torque $T_{e,des}$ to the desired throttle command $\tau_{t,des}$. As the torque map is built as a lookup table, we search the desired throttle with respect to a given engine speed and desired torque. The inverse brake model is a module to convert the braking force to the brake pedal command, which is activated if $F_{x,r}$ is negative. The brake model is also attained by our proposed MIHO, but details are omitted to conserve space.

C. Model-based Path Tracking Control

We follow the lateral vehicle dynamics of [14] illustrated in the right of Fig 2. The lateral model is derived from the objective of tracking a reference trajectory. We implement path tracking control by stabilizing a velocity-dependent chassis model in terms of the error state variables ξ and control u .

$$\xi = [e_y, \dot{e}_y, e_\psi, \dot{e}_\psi]^T, \quad u = \delta, \quad (13)$$

where e_y, e_ψ denote the position and orientation error with respect to a given trajectory. The lateral model contains tire-related model parameters such as the cornering stiffnesses of the front and rear tires $C_{\alpha,f}, C_{\alpha,r}$. Since the lateral dynamics is obtained from the bicycle model, the front and rear tire models are optimized according to Eq 4, but the sum of the left and right tire forces is used as the model output. The cornering stiffnesses then can be approximated as follows [14]:

$$C_{\alpha f} \approx B_f \times C_f \times D_f, \quad C_{\alpha r} \approx B_r \times C_r \times D_r. \quad (14)$$

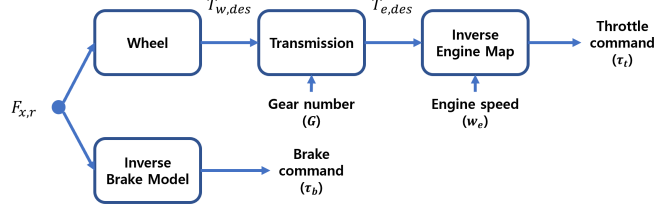


Fig. 3. Throttle and brake control system.

Based on the lateral vehicle model, we design the Linear Quadratic Regulator with the following optimization problem:

$$\min_u \int_0^\infty (\xi^T Q \xi + u^T R u) dt, \quad (15)$$

where Q, R denote gain matrices for LQR. For the real-time control performance, we compute the state feedback optimal LQR gains over piecewise velocity intervals offline [21].

V. EVALUATION

A. Analysis for Model Identification

1) *Tire Dynamics Model*: Fig. 4 illustrates the learned tire models with datasets provided as the tire property files (*.tir). The files contain tire force and moment characteristics with high fidelity [22]. For model identification, we sampled 3000 data for each tire using the property files in various tire state conditions such as tire load, camber angle, slip angle, and slip ratio. As illustrated in the left and middle of Fig. 4, the learned models show good fitness to the tire characteristic distribution. We further investigated the tire model with the test drive data collected during track racing. The right of Fig. 4 illustrates the front tire model of the single-track bicycle dynamics learned by the provided tire property data comparing it with the driving data that is not used for learning. The learned model shows the generalization ability for the overall data distribution represented by blue dots. However, since we obtained the model by offline optimization and focused on the representativeness of data, the model needs higher accuracy in some edge cases near the peaks of the lateral force. To handle these cases, an online parameter optimization can be used by parallelizing the HPO process in MIHO, and we will implement it in future work.

2) *Engine Torque Model*: Fig. 5 illustrates the learned engine torque curves and integrated engine map. The data for the engine map was provided by engine dynamometer testing. For higher reliability, we incorporated our data-driven engine torque models with the dyno data, especially for the throttle pedals 5, 15, and 20%, where the dynamometer showed insufficient accuracy in torque measurements. The result shows that the learned torque curves are able to represent the change of the maximum torque according to the throttle commands. Moreover, the learned models also fit the torque curves that change nonlinearly as a function of engine speed. We integrated the learned torque models with the provided dyno data and interpolated the torque data to construct an engine lookup table. The blue area on the right of Fig 5 shows the interpolated region by the learned torque curves. Our vehicle utilized the learned region in racing scenarios such as pit-in/out, obstacle avoidance, and driving within 100km/h (Fig. 7).

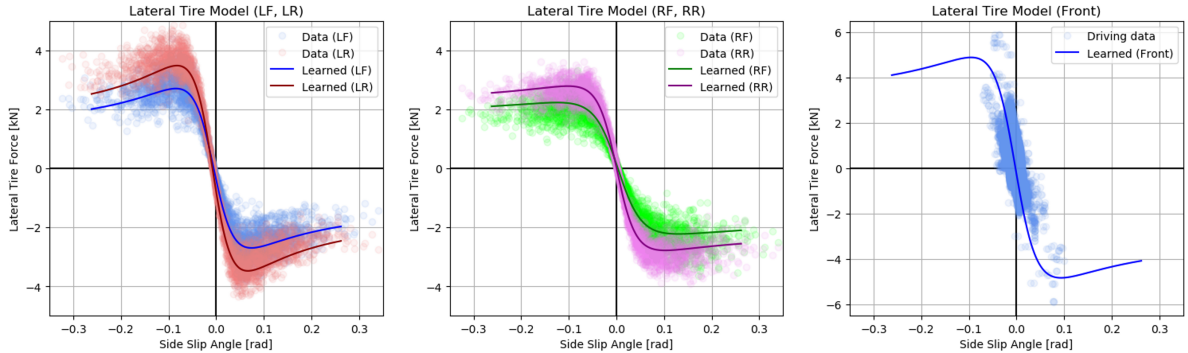


Fig. 4. Learned tire models with the provided tire data (Left: left-front and right-front, Middle: left-rear and right-rear). Right: Learned front tire dynamics of the single-track bicycle model and the distribution of the collected data on the track.

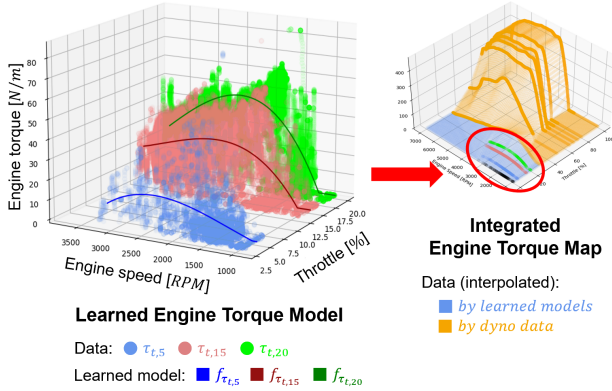


Fig. 5. Learned engine torque curves and the integrated engine map.

B. Control Performance in Indy Autonomous Challenge

Our model-based planning and control algorithms were deployed in the full-scale racecar platform. Moreover, we extensively validated our learned model parameter-based algorithms in the real-world race tracks, IMS and LVMS. The algorithms successfully performed various race scenarios, such as obstacle avoidance and high-speed autonomous driving over 200km/h on the race tracks (Fig. 6).

1) *Obstacle Avoidance at the IMS*: Fig. 7 shows the quantitative results of the obstacle avoidance mission. In this mission, obstacles are located before the first-corner section, where the velocity plan is critical for avoiding collision while keeping close to the racing line. For the sake of safety, we set the tire performance factor μ as 0.7. Our dynamics-aware velocity planner was able to allow the racecar to maximize the velocity while regulating the lateral acceleration within the learned maximum tire performance during the rapid avoidance maneuvers. The obstacle avoidance was initiated in high-speed driving at 100km/h, and steering commands were computed up to -10 degrees to follow the generated collision-free reference trajectory. The sharp steering command could cause significant lateral acceleration higher than $9.0m/s^2$, which might cause critical tire grip loss. However, our tire model-based velocity planner inferred the allowable maximum lateral acceleration based on the real-time tire load. As a result, it was possible to plan for safe desired velocity within lateral acceleration limit capable of preserving the tire grip performance.

2) *High-Speed Autonomous Driving in LVMS*: Furthermore, we extensively validated the control performance based on the optimized model parameters at LVMS. Fig. 8 illustrates the quantitative results of the lateral and longitudinal control while our vehicle raced more than nine laps (23km). Our path-tracking algorithm shows robust control performance leveraging the learned tire parameters. The largest position and orientation errors were 0.6m and -2.2 degrees, respectively. In addition, the AV-21 succeeded high-speed autonomous driving at above 144km/h (with a top speed of 217.4km/h), where the dynamic scenario had yet to be visited and adjusted before this track experiment. These results demonstrate that MIHO can optimize and provide appropriate prior dynamics models offline for the design of model-based control before deployment. However, the characteristic of vehicle dynamics changed and affected the control performance over high-speed driving. As shown in the bottom of Fig. 8, the tire temperatures were increased after reaching the unseen velocity range. In addition, after visiting the range of over 144km/h, our low-level controller computed throttle command of over 50% with the engine range consisting only of the provided dyno data. Those factors might have an effect on the velocity error in the velocity range [42, 52]m/s of Fig. 8. Nevertheless, the control system can be improved with an extended data-driven engine map for throttle control at high-speed. We also point out that our method has the potential to be processed online by parallelizing the HPO process [9], which enables the method to identify the model in real-time during deployment. The online MIHO could be incorporated with the offline model optimization introduced in this work, and we leave it as an important future work.

VI. CONCLUSION

We present MIHO, a data-driven model identification method via hyperparameter optimization. Our approach showed the ability to optimize the parameters of the dynamics models, such as the tire models and engine torque curves. Furthermore, the model-based planning and control system with the learned model parameters demonstrated stable performance in the real-world track environments, IMS and LVMS. In future works, we will implement the online HPO method and integrate it with the offline method of this work to iteratively infer the changing parameters of the vehicle dynamics while on track.

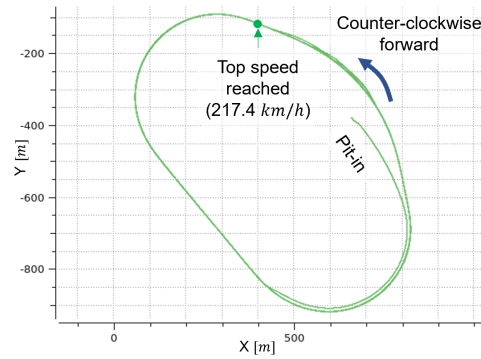
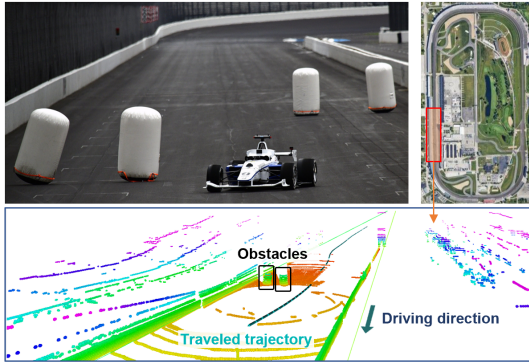


Fig. 6. **Left:** Team KAIST's successful obstacle avoidance at IMS. The bottom illustrates the point cloud data and traveled trajectory during avoidance. **Right:** Our AV-21 drove more than nine laps (23km) at the Tri-Oval Superspeedway of LVMS.

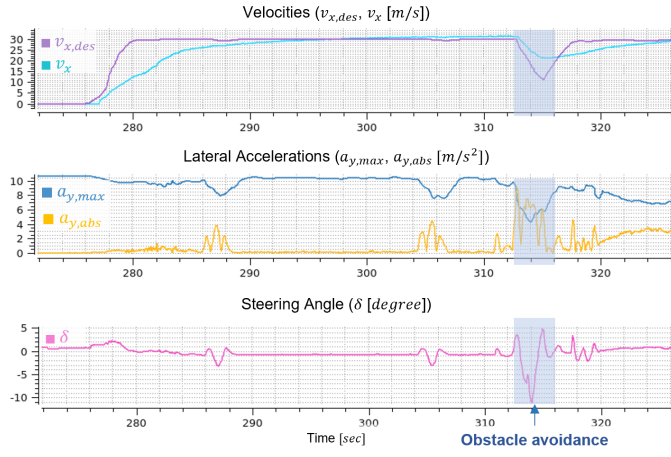


Fig. 7. Results of the velocity control, lateral accelerations, and steering angles during the obstacle avoidance mission at the IMS.

REFERENCES

- [1] F. L. Lewis, D. Vrabie, and V. L. Syrmos, *Optimal control*. John Wiley & Sons, 2012.
- [2] C. Jung, S. Lee, H. Seong, A. Finazzi, and D. H. Shim, “Game-theoretic model predictive control with data-driven identification of vehicle model for head-to-head autonomous racing,” *arXiv preprint arXiv:2106.04094*, 2021.
- [3] A. K. Tangirala, *Principles of system identification: theory and practice*. Crc Press, 2018.
- [4] S. L. Brunton and J. N. Kutz, *Data-driven science and engineering: Machine learning, dynamical systems, and control*. Cambridge University Press, 2022.
- [5] N. A. Spielberg, M. Brown, N. R. Kapania, J. C. Kegelman, and J. C. Gerdes, “Neural network vehicle models for high-performance automated driving,” *Science robotics*, vol. 4, no. 28, p. eaaw1975, 2019.
- [6] L. Hermansdorfer, R. Trauth, J. Betz, and M. Lienkamp, “End-to-end neural network for vehicle dynamics modeling,” in *2020 6th IEEE Congress on Information Science and Technology (CiSt)*. IEEE, 2021, pp. 407–412.
- [7] Energy Systems Network, “Indy autonomous challenge,” 2022. [Online]. Available: www.indyautonomouschallenge.com
- [8] M. Feurer and F. Hutter, “Hyperparameter optimization,” in *Automated machine learning*. Springer, Cham, 2019, pp. 3–33.
- [9] L. Li, K. Jamieson, G. DeSalvo, A. Rostamizadeh, and A. Talwalkar, “Hyperband: A novel bandit-based approach to hyperparameter optimization,” *The Journal of Machine Learning Research*, vol. 18, no. 1, pp. 6765–6816, 2017.
- [10] S. Mirjalili, “Genetic algorithm,” in *Evolutionary algorithms and neural networks*. Springer, 2019, pp. 43–55.
- [11] S. Kirkpatrick, C. D. Gelatt Jr, and M. P. Vecchi, “Optimization by simulated annealing,” *science*, vol. 220, no. 4598, pp. 671–680, 1983.
- [12] E. Bakker, L. Nyborg, and H. B. Pacejka, “Tyre modelling for use in vehicle dynamics studies,” *SAE Transactions*, pp. 190–204, 1987.
- [13] J. Kabzan, M. I. Valls, V. J. Reijgwart, H. F. Hendrikx, C. Ehmke, M. Prajapat, A. Bühl, N. Gosala, M. Gupta, R. Sivanesan *et al.*, “Amz driverless: The full autonomous racing system,” *Journal of Field Robotics*, vol. 37, no. 7, pp. 1267–1294, 2020.
- [14] R. Rajamani, *Vehicle dynamics and control*. Springer Science & Business Media, 2011.
- [15] L. Li, Z. Zhu, X. Wang, Y. Yang, C. Yang, and J. Song, “Identification of a driver’s starting intention based on an artificial neural network for vehicles equipped with an automated manual transmission,” *Proceedings of the Institution of Mechanical Engineers, Part D: Journal of Automobile Engineering*, vol. 230, no. 10, pp. 1417–1429, 2016.
- [16] J. S. Killeen, *Dynamometer: theory and application to engine testing*. Xlibris Corporation, 2012.
- [17] D. Seward, *Race car design*. Bloomsbury Publishing, 2017.
- [18] D. Lee, C. Jung, A. Finazzi, H. Seong, and D. H. Shim, “Resilient navigation and path planning system for high-speed autonomous race car,” *arXiv preprint arXiv:2207.12232*, 2022.
- [19] J. C. Doyle, B. A. Francis, and A. R. Tannenbaum, *Feedback control theory*. Courier Corporation, 2013.
- [20] K. Hedrick *et al.*, “Brake system modeling, control and integrated brake/throttle switching phase i,” 1997.
- [21] J. Spisak, A. Saba, N. Suvarna, B. Mao, C. T. Zhang, C. Chang, S. Scherer, and D. Ramanan, “Robust modeling and controls for racing on the edge,” *arXiv preprint arXiv:2205.10841*, 2022.
- [22] A. Schmeitz, “Mf-tyre/mf-swift,” *Delft: TNO*, 2013.

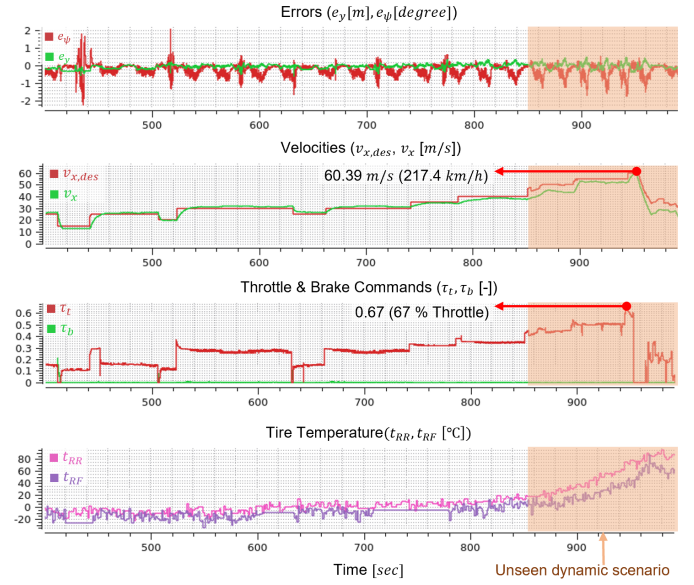


Fig. 8. Results of the errors, velocity control, throttle/brake controls, and temperature of the right-rear and right-front tires in LVMS.